

Smectic membranes in aqueous environment

Yasutaka Iwashita,^{1,*} Stephan Herminghaus,¹ Ralf Seemann,^{1,2} and Christian Bahr¹

¹Max Planck Institute for Dynamics and Self-Organization, 37073 Göttingen, Germany

²Experimental Physics, Saarland University, 66041 Saarbrücken, Germany

(Received 16 March 2010; published 21 May 2010)

We present a study of thermotropic smectic liquid crystal films in aqueous environment. Macroscopic freely suspended films in water with a size up to $7.4 \times 15 \text{ mm}^2$ were prepared with the help of a surfactant, which ensures a strong homeotropic anchoring at liquid crystal/water interfaces. The films were studied by optical microscopy and ellipsometry. Attention was paid to the stability and the thinning transitions which occurred at temperatures above the bulk smectic-A-isotropic transition temperature. In addition, we investigated the formation and rupture kinetics of thin smectic membranes separating water droplets in microfluidic devices. Besides possible applications in discrete microfluidics, smectic films in aqueous environment may expand the general range of possible studies of freely suspended smectic films.

DOI: [10.1103/PhysRevE.81.051709](https://doi.org/10.1103/PhysRevE.81.051709)

PACS number(s): 61.30.Hn, 64.70.mj

I. INTRODUCTION

Thermotropic smectic liquid crystals (LCs) easily form thin films which are freely suspended on a solid frame in air [1–5]. These systems have been studied for various purposes: clarifying the structure of smectic phases [6–9], investigating phase transitions in two-dimensional systems [10–12], and studying various physical properties of liquid crystals [13–18]. These studies are based mainly on two useful features of freely suspended smectic films: they show an almost perfect defect-free order of the smectic layers, arranged parallel to the two surfaces of the film, and their thickness can be tuned from a thick three-dimensional state ($\approx 100 \text{ }\mu\text{m}$) to a two-dimensional one (down to only two smectic layers $\approx 5 \text{ nm}$). Furthermore, various smectic subphases and phase transitions between them are available and the films are fairly stable.

The two parameters that differentiate a film from its bulk are thickness and surface properties such as surface tension and anchoring. The thickness determines the degree of two dimensionality of the system and the surface properties become more dominant over the behavior of the sample in a thinner film. In a freely suspended LC film in air, however, it is almost impossible to control or to modify the surface properties in a given system, since there are almost no surface-active agents at nonpolar liquid/air interfaces. This imposes a certain limitation to the studies of films suspended in air (whereas controlling the thickness is not difficult).

In the present study, we report on the preparation of freely suspended smectic films in water [Fig. 1(a)]. Most LC molecules tend to align planar at the interface to an immiscible liquid such as water, thereby preventing the generation of freely suspended films in their usual configuration in which the smectic layers are parallel to the two film surfaces. However, a homeotropic anchoring at LC/water interfaces can be attained by the use of suitable surfactants [19]. Moreover, by controlling the amount of surfactant adsorbed at the interface, it is also possible to tune the anchoring strength, i.e.,

the strength of the ordering surface field [20–22]. Thus, the preparation of freely suspended smectic films in an aqueous environment may expand the range of possible studies of these systems considerably. We show that macroscopic freely suspended smectic films with an area of $\approx 1 \text{ cm}^2$ can be prepared and we study their behavior in the temperature range a few $^\circ\text{C}$ above the smectic-A-isotropic bulk transition; in this temperature range, the presence of surface-induced smectic order at single surfactant-laden LC/water interfaces has been demonstrated [21]. The smectic surface order appears to provide a certain stability to thin (a few smectic layers) freely suspended films above the smectic-A-isotropic

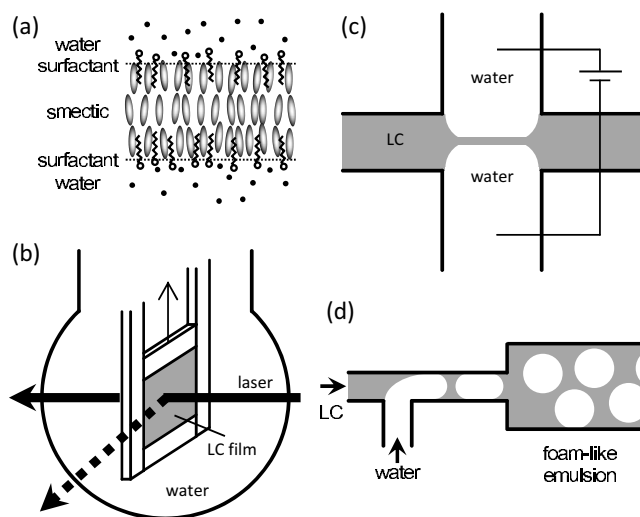


FIG. 1. Schematics of a smectic film and setups. (a) The cross section of a freely suspended smectic film in water. (For clarity, the smectic layers are drawn as simple monolayers whereas nCB compounds show in fact a partial double layer structure [25].) (b) A Teflon frame with a mobile chariot in a flask filled with water. The angle of the laser for ellipsometry (solid arrow) to the film is fixed at 45° . The beam reflected by the film (dotted arrow) was also observed. (c) The setup for electrocoalescence. The two tips of the water phases meet at the center which was filled with the LC sample. (d) A microfluidic device for producing a foamlike structure composed of water droplets separated by LC films.

*Present address: Kyushu University, 812-8581 Fukuoka, Japan.

bulk transition. Besides macroscopic freely suspended films, we study smectic membranes separating water droplets in microfluidic devices. Similar to the behavior of the macroscopic films, the stability of the microfluidic smectic membranes changes significantly within a small temperature range above the smectic-A-isotropic bulk transition. This behavior could lead to new applications in discrete microfluidics [23].

II. EXPERIMENT

A. Sample

The LC compounds used were decylcyanobiphenyl (10CB) and dodecylcyanobiphenyl (12CB) (Synthon Chemicals), which possess a smectic-A-isotropic phase transition at a temperature $T_{AI}=50$ °C (10CB) and 59 °C (12CB). The LCs were doped with a small amount of a surfactant, 1-oleoylglycerol (mono-olein) (Fluka). The molar fraction of the surfactant in the LC bulk phase, ρ_s , was on the order of 0.05, ensuring a strong homeotropic anchoring potential at the LC/water interface. Similar to observations at LC/air interfaces [24], the homeotropic anchoring at surfactant-laden LC/water interfaces leads to surface-induced order, i.e., in a temperature range of a few °C above T_{AI} , a smectic surface phase, consisting of a few smectic layers, exists at the interface between the isotropic liquid crystal and the aqueous phase. The number of smectic layers increases as T_{AI} is approached [21]. Note that T_{AI} for the LC/mono-olein mixtures is 2–3 °C lower than for pure 10CB and 12CB. In the following, temperatures are occasionally given relative to T_{AI} , i.e., by $\Delta T=T-T_{AI}$.

B. Setups

We used three setups for different experiments. The first one is a Teflon frame for forming large freely suspended LC films [Fig. 1(b)]. The frame has a mobile chariot that controls the height h of the aperture while the aperture's width was fixed at $w=7.4$ mm. The motion of the chariot was driven by a computer-controlled stepping motor or manual rotation of a screw connected to the chariot. The closed frame was loaded with the LC sample and then inserted into a spherical glass flask filled with water. The wettability of nCB compounds to Teflon is better than that of water. The flask was put into a temperature-controlled copper box (accuracy 0.1 °C) possessing windows for optical microscopy and ellipsometry. The temperature of the sample was measured by a thermistor placed on the Teflon frame near the aperture. Experiments were done after the system reached a constant temperature, or with a small temperature rate on the order of 0.05 °C/min.

The second setup was a microfluidic device enabling a “side view” of a film while measuring its stability by electrocoalescence [Fig. 1(c)] [26]. A dc voltage was applied across the film that separated two Millipore water phases. If the electric field reaches a certain strength, the film ruptures and the water phases coalesce [26,27]. The two liquids (LC and water) were in a microfluidic device with two straight channels forming a rectangular junction at the center. The

gold electrodes that contacted to the two water phases were evaporated on the top plate of the device. The positions of the LC/water interfaces were controlled precisely by syringe pumps, and the water phases were replaced after each measurement to avoid possible bias by ionic impurities. The LCs completely wet the surface of the microfluidic device made of poly(methyl methacrylate) (PMMA).

The third setup was a PMMA microfluidic device which we used for the generation of a foamlike structure in which water droplets are separated by thin liquid crystal membranes [Fig. 1(d)] [28]. The channels which dimensions of the order of 0.1–1 mm were micromachined. The flow rates of water and LC were controlled by syringe pumps and water droplets, separated by LC films, were produced at the T-junction of the channels. The water droplets formed a foamlike structure which was flowing into a larger channel where the coarsening process was observed after both flows (water and LC) were stopped. The microfluidic device was located in a temperature-controlled copper box (accuracy of ≈ 0.1 °C).

C. Optical observation and ellipsometry

The microfluidic setups and the macroscopic films suspended on the Teflon frame were observed by optical microscopy. In addition, ellipsometry measurements were conducted on the macroscopic freely suspended films. A null ellipsometer (Optrel Multiskop), equipped with a He-Ne laser ($\lambda=632.8$ nm), was used in transmission geometry (angle of incidence $\theta_i=45^\circ$). An ellipsometric measurement consists of the determination of two parameters, Δ and Ψ , which describe the polarization of the transmitted light. Here, Δ corresponds to the phase difference between the s - and p -polarized light components, and $\tan \Psi$ gives the ratio of the amplitudes of the two components. The polarization of the incident light is described by $\Delta=0$ and $\tan \Psi=1$.

A freely suspended smectic-A film corresponds to a thin optically uniaxial film with its optical axis oriented perpendicular to the film plane. For such an optical system, Δ and Ψ show a characteristic dependence on the film thickness d . While $\Psi(d)$ oscillates with a purely sinusoidal shape, $\Delta(d)$ is the superposition of a linearly decreasing part (the slope of which being a measure of the birefringence of the smectic-A phase) and an oscillating sinusoidal part. An example for $\Psi(d)$ and $\Delta(d)$ for a freely suspended smectic-A film in air is given in [29]. For a freely suspended film in water, the oscillatory part in $\Delta(d)$ is considerably decreased, and $\Delta(d)$ becomes a monotonically decreasing function of d . To calculate $\Psi(d)$ and $\Delta(d)$ for 10CB, we used the refractive index values given in [30] ($n_e=1.645$, $n_o=1.50$) and the refractive index of water was set to $n_w=1.33$. Equations for the calculation of $\Psi(d)$ and $\Delta(d)$ are given in [29,31].

III. RESULTS

A. Macroscopic freely suspended smectic films in water

We prepared macroscopic freely suspended films of 10CB and 12CB. Both compounds showed essentially the same behavior. In the following, we describe our observations for

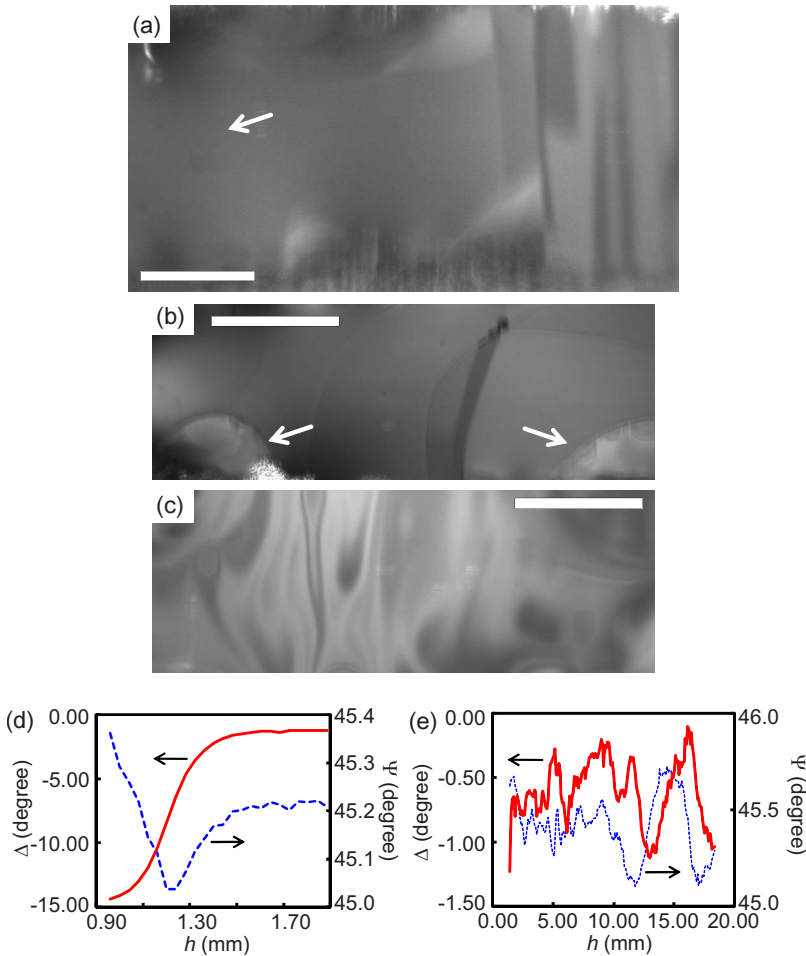


FIG. 2. (Color online) Reflection microscopy images and ellipsometry data of freely suspended 10CB films. The images are blurred vertically because of small corrugations in the glass walls of the flask. In the graphs, red thick solid lines correspond to Δ and blue dashed lines correspond to Ψ , respectively. (a) A thick smectic film being vertically expanded with $v=5 \mu\text{m/s}$ at $h=1.48 \text{ mm}$ and $\Delta T=-1.0 \text{ }^\circ\text{C}$. The arrow indicates the position of the laser for ellipsometry. The upper and lower edge of the Teflon frame are in the image. (b) Thick smectic film at $\Delta T=0.0 \text{ }^\circ\text{C}$ on heating at $0.05 \text{ }^\circ\text{C/min}$ and $h=1.76 \text{ mm}$. Near the meniscus, the phase transition from smectic-A to isotropic starts (the isotropic phase is indicated by the arrows). (c) A film at $\Delta T=0.6 \text{ }^\circ\text{C}$ and $h=5.3 \text{ mm}$ after the transition to the isotropic phase. The heterogeneity is probably due to convective flows in the film caused by its shrinkage at $v=12.5 \mu\text{m/s}$. (d) Ellipsometric parameters of the thick smectic film in (a) measured against the film height during the expansion. (e) Ellipsometric parameters of an isotropic film measured during expansion. Scale bars are 0.5 mm in (a) and 1.0 mm in (b) and (c).

10CB, which we studied in somewhat more detail than 12CB.

In order to prepare freely suspended smectic films on the Teflon frame, a few mg of a 10CB/mono-olein mixture (surfactant mol fraction $\rho_s=0.062$) were put on the closed aperture of the frame. The frame was heated in air above T_{AI} and the isotropic sample was allowed to wet the closed aperture. Then, the frame was put into the flask, which was filled with water with a temperature of $\sim 5-10 \text{ }^\circ\text{C}$ above T_{AI} . The temperature was lowered to the range of the bulk smectic-A phase and the aperture was opened at a constant rate v (typically a few $\mu\text{m/s}$), resulting in the formation of a freely suspended smectic film [Fig. 2(a)]. When observed in white light, the film showed a step-like pattern with different intensities of the reflected light. The pattern, which was anisotropic during the expansion of the film, coarsened with time. These observations are also characteristic for freely suspended smectic films in air [2]. The different reflection intensities result from regions possessing different thicknesses, i.e., consisting of different numbers of smectic layers.

During the expansion of the film, the thickness of the film was decreasing. The ellipsometric parameter Δ increased monotonically while Ψ first decreased and then increased again [Fig. 2(d)] as expected for the thinning of a uniaxial film in water (cf. Sec. II C). From the data of Fig. 2(d), we can calculate that the film thickness d decreased from ≈ 400 to 50 nm .

Thick ($0.1-1 \mu\text{m}$) freely suspended smectic films were fairly stable. The film in Fig. 2(a) was stable for several expansion and shrinking cycles between $h \approx 0$ and 15 mm at $v \approx 10-50 \mu\text{m/s}$. Large films with an area of $7.4 \times 10 \text{ mm}^2$ and a thickness $\approx 0.1-1 \mu\text{m}$ were stable for more than 12 h. We should note that we did not make a special effort to isolate our setup from disturbances due to the environment. Compared to freely suspended films in air, films in water are surrounded by a medium possessing a three orders of magnitude larger density; therefore, a convection of the water or a small movement of the frame have a much larger effect on the film stability. To destroy the film intentionally, it was sufficient to give a small mechanical flip to the frame. On the other hand, the reduced surface tension due to the presence of the surfactant at the LC/water interface might provide some stability to the film even when the smectic layer structure is gone. This is supported by the recent observation that it is possible to prepare thick ($\approx 100 \mu\text{m}$) freely suspended nematic films in water, provided a surfactant is present [32,33]. In air, freely suspended nematic or isotropic films are not stable. Accordingly, freely suspended smectic films are usually destroyed when heated to the nematic or isotropic phase; a small number of compounds possessing partially perfluorinated alkyl chains show a regular layer-by-layer thinning process [34] but films of nCB compounds just rupture when heated above the smectic-A phase range. Thus, it seemed interesting to study

the behavior of our macroscopic smectic films in water on heating to the isotropic temperature range.

When we heated a smectic 10CB film at a rate $Q = 0.05$ °C/min, first indications of the isotropic phase appeared at $T = T_{AI}$ at the meniscus of the film [Fig. 2(b)]. At $\Delta T \approx 0.3$ °C, the complete film was transformed into the isotropic phase: the sharp boundaries between regions of different reflectivity (different thickness) had vanished and the reflectivity changed smoothly across the film [Fig. 2(c)]. The isotropic nature of the film is also shown by ellipsometry [Fig. 2(e)]: When the isotropic film was expanded, i.e., its thickness decreased, Δ did not show a monotonic increase but rather an oscillating behavior between the values of -1.25° and -0.25° (the small noiselike fluctuations of the film thickness). This oscillation qualitatively coincides with the calculated $\Delta(d)$ curve for an isotropic, nonbirefringent film although the calculated $\Delta(d)$ curve oscillates around 0° and with a somewhat larger amplitude. The shift to negative Δ values could be due to smectic surface layers, which are present at the isotropic LC/water interface even above T_{AI} [21]. As will be explained below, a few smectic layers on both sides of a film can shift Δ by $\approx -0.5^\circ$. The thick ($0.1\text{--}1$ μm) isotropic films were less stable than the smectic films with a similar thickness: often they ruptured within ≈ 10 min after the temperature was raised above T_{AI} . In several cases, however, the films remained stable and we could observe a specific thinning behavior described below. The thick isotropic films should have a structure similar to the membrane of a water-surfactant-oil ternary system, though we did not study how stable our isotropic membranes could be and how they were stabilized.

If the isotropic films did not rupture after the temperature was raised above T_{AI} , the following thinning behavior was observed on further heating: With increasing temperature, first a sudden thinning process occurred. During this one-step thinning process, most of the isotropic LC material left the film and was absorbed to the meniscus [Fig. 3(a)], but a thin film with very low reflectivity remained. An optical inspection of this thin film shows again a steplike pattern [Fig. 3(b)], similar to that observed for the thick films in the bulk smectic-A temperature range. From the image and formation process, this film is considered to be a thin smectic film stabilized by surface ordering effects above the smectic-A-isotropic transition point T_{AI} [21]. A schematic of this thin film formation process is shown in Fig. 3(c).

After the one-step thinning of the thick isotropic film, a layer-by-layer thinning process occurred with increasing temperature until the thin films ruptured (indicated by the vanishing of the laser beam reflected from the film) ≈ 2 °C above the bulk smectic-A-isotropic transition. The layer-by-layer thinning is demonstrated by the ellipsometry data shown in Fig. 4(a). With increasing temperature, Δ increases in a steplike fashion while Ψ shows a similar but decreasing behavior. At $\Delta T = 1.9$ °C, the film ruptured and for Δ and Ψ the values of the incident light (0° , respectively, 45°) are obtained. We numbered the plateaus of constant Δ and Ψ with values from 0 to 9, where 0 corresponds to the data measured after the rupture of the film. We should note that narrow plateaus are still distinguishable: The narrowest one,

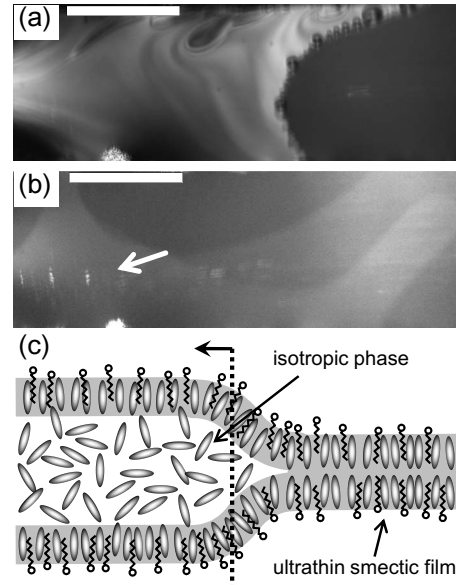


FIG. 3. Formation of a thin freely suspended film above T_{AI} . (a) Removal of the isotropic phase (gray areas) from right to left at $\Delta T = 0.7$ °C on heating at $Q = 0.05$ °C/min. The upper edge of the frame is almost at the top of the image. (b) Thin smectic film after the one-step thinning process. $\Delta T = 1.9$ °C and $Q = 0.05$ °C/min. The contrast is largely enhanced. According to the value of $\Delta = -0.31^\circ$ at the arrowed point, the thickness amounts to ≈ 14 nm (see text). Scale bars are 1.000 mm in (a) and (b). (c) Schematic cross-section of the film during the thin film formation process. The shadowed regions are the surface smectic layers, that is one layer in this figure.

plateau 3, is composed of six data points, which is somewhat larger than the typical wavelength of noisy fluctuation, one to two points. This assignment of plateaus is also supported by the coincidence of the values of plateaus with the theoretical calculation in the next paragraph.

Figure 4(b) shows the averaged Δ and Ψ values measured for the plateaus 1 to 9 in Fig. 4(a) together with the theoretically calculated Δ and Ψ curves as a function of film thickness i in units of smectic layer numbers (thickness of a single smectic layer = 3.5 nm [30]). Here the averaging Ψ is simply done in the range of the plateaus of Δ . The standard errors of the averaging Δ and Ψ are rather small since the numbers of data points of the plateaus are enough compared with the amplitude of the noise; the maximum error of $\Delta(i)$ is 0.006° for $i = 1$, which is roughly 10% of the change of the plateau height, and that of $\Psi(i)$ is 0.003° for $i = 4$, which is about a half of the change of the plateau height around $i = 4$.

Obviously, the averaged Δ and Ψ values coincide well with the calculated values for films consisting of one to nine layers. This result strongly suggests that each step in the measured Δ and Ψ data corresponds to the thinning of the film by a single smectic-A layer. For the small deviation between the measurement and theory, it could be explained by the small uncertainties of experimental conditions such as the geometry of the setup and refractive index of the sample.

If the heating of the film was stopped just after the one-step thinning process, the thin (thickness of ≈ 10 layers) film with a size 7.4×2 mm² could retain itself more than one

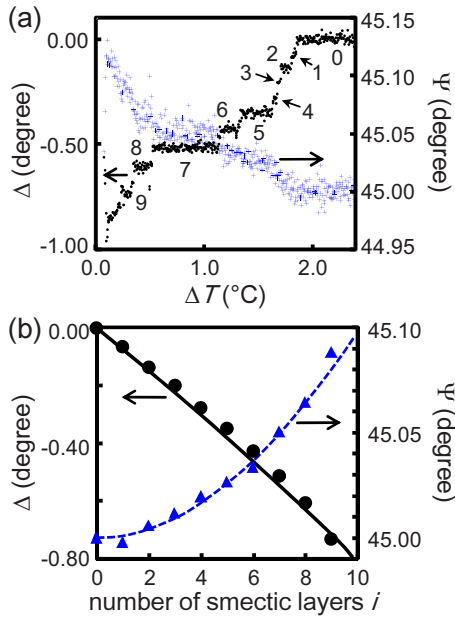


FIG. 4. (Color online) (a) Ellipsometric parameters of a thin 10CB film on heating at $0.05\text{ }^\circ\text{C}/\text{min}$ and $h=2.0\text{ mm}$. Black dots are values of Δ and blue crosses are values of Ψ , respectively. The numbers indicate plateaus of constant Δ and Ψ values (counted from the final plateau that was measured after the rupture of the film). (b) Comparison between the measured parameters, Δ (black circle) and Ψ (blue triangle), and their calculated values (black solid and blue dashed curve) for a smectic film in which i corresponds to the number of smectic layers of the film.

hour once it was formed, though the layer-by-layer thinning might proceed slowly compared to that at higher temperature. We note that a thickness of ten layers is larger than the sum of the surface-ordered smectic layers measured at isolated isotropic LC/water interfaces: at temperatures $0.5\text{--}1.0\text{ }^\circ\text{C}$ above T_{AI} , just one or two smectic layers were observed [21]. The stability of films with ≈ 10 layers might indicate the presence of a capillary condensation effect caused by the small distance of the two LC/water interfaces of the film; such an effect has already been observed near a nematic-isotropic transition [35].

On the other hand, the stability of the thin (ten layers and less) films above T_{AI} was clearly inferior to that of the thick ($0.1\text{--}1\text{ }\mu\text{m}$) smectic films below T_{AI} . Often, a film ruptured during the one-step thick to thin transition. We would need more statistical data to make a statement about the quantitative determination of the thinning temperatures and their reproducibility. The thick to thin transition and the subsequent single layer thinning transitions varied within a certain range from experiment to experiment. For instance, the one-step thinning process was observed $0.5 \pm 0.3\text{ }^\circ\text{C}$ above T_{AI} in about 10 runs and the temperature tended to be higher for a faster heating rate.

B. Formation and rupture kinetics of smectic membranes in microfluidic channels

For studying the formation and rupture process of smectic films in more detail, we used a microfluidic device, the

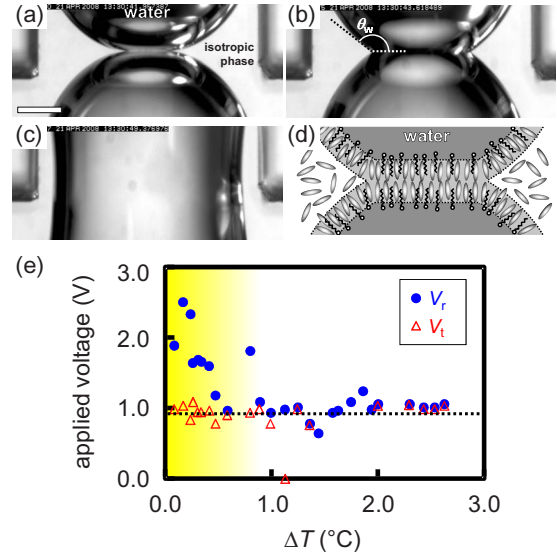


FIG. 5. (Color online) Rupture kinetics studied by electrocoalescence in a microfluidic device. Micrographs (a) to (c) show the rupture process of a LC film formed between two water tips (the darker phases in the images) at $\Delta T=0.3\text{ }^\circ\text{C}$. The time elapsed after applying voltage started was 9.4, 11.1, and 16.8 s, respectively, for (a)–(c). The LC sample was 12CB with $\rho_s=0.05$, the scale bar corresponds to $200\text{ }\mu\text{m}$. (d) A schematic of a smectic film between water tips. The light gray area corresponds to the surface smectic-ordered layers. (e) Temperature dependence of the voltage V_t (red triangle) at which the angle θ_w , defined in (b), changed from $\approx 180^\circ$ to $\approx 142^\circ$, and of the voltage V_r (blue circle) at which the films ruptured. When a film ruptured without a change of θ_w in the observation, only V_r is plotted.

second setup described in Sec. II B. First, the channels were filled with an isotropic 12CB/mono-olein mixture ($\rho_s=0.05$) at a temperature a few degrees above T_{AI} . Then, using precise syringe pumps, we let two water phases with almost hemispherical tips approach each other at the crossing of the channels until they touched each other and a thin LC film formed between them. The pumps were stopped to hold the film area and position constant and then a linearly increasing voltage at a rate of 0.1 V/s was applied across the LC film until the film was destroyed. Figures 5(a)–5(c) illustrates our observations for a typical rupture process: After the contact of the water tips, we observed first a state in which the angle of the water phase to the film, θ_w , was $\approx 180^\circ$, i.e., the LC wetted the water completely [Fig. 5(a)]. Then, at a certain voltage, θ_w suddenly jumped to $\approx 142^\circ$ [Fig. 5(b)]. Finally, on further increasing the voltage, the film ruptured [Fig. 5(c)]. However, at temperatures higher than $\approx 1\text{ }^\circ\text{C}$ above T_{AI} , the state with $\theta_w \approx 142^\circ$ was sometimes not observed, i.e., the films with $\theta_w \approx 180^\circ$ ruptured directly.

Figure 5(e) shows the temperature dependence of the voltage V_t , at which the transition of θ_w from 180° to 142° occurred, and the voltage V_r , at which the films ruptured. To understand these results, we first consider what occurs at V_t : At this voltage, we observed that a circular patch nucleated and grew, accompanied by a flow of material toward the meniscus, resembling the observations on the macroscopic

thick isotropic films [Fig. 3(a)]. The value $\theta_w = 180^\circ$ implies that there is no difference between the interfacial tensions at the water/LC film and water/isotropic LC bulk reservoir interface. Thus, the change of θ_w should be due to the one-step thinning process described in Sec. III A and the film which is left after the change of θ_w to 142° should correspond to the thin (ten layers or less) smectic film shown in Fig. 3(b). In this model, the observed increase of V_r toward T_{AI} ($\Delta T = 0^\circ\text{C}$) would be a result of the increasing thickness of the thin smectic film due to the increasing surface order near T_{AI} . The temperature range in which the increase of V_r is observed ($\Delta T < 0.7^\circ\text{C}$) corresponds approximately to the range in which at least two smectic layers exist at the interface between the isotropic LC and the aqueous phase [21]. The large scatter of the data is presumably due to the probabilistic nature of the rupture.

At higher temperatures ($\Delta T > 1^\circ\text{C}$), the films ruptured immediately after the change of the angle θ_w . In some cases, it was not possible to decide if a film with $\theta_w = 180^\circ$ ruptured directly or if there was a preceding change of θ_w because the stability time of the film with $\theta_w = 142^\circ$ was similar to the used video frame rate (1/30 s). At single LC/water interfaces, the 12CB sample with $\rho_s = 0.05$ shows one smectic surface layer for $0.7 < \Delta T < 2.5$ (and no surface order at higher temperatures) [21]. The observations described above indicate that this low surface order is not sufficient to stabilize thin films and the films rupture almost at the instance at which the films with $\theta_w = 180^\circ$ become unstable.

The observation that the voltage V_r at which the angle θ_w changes its value is independent from temperature could be explained if we assume that the films with $\theta_w = 180^\circ$ are just μm -thick isotropic LC films as suggested above. A temperature change of a few $^\circ\text{C}$ as well as the presence of a nanometer-thick ordered surface layer hardly influence the rheological and dielectric properties of thick isotropic LC films, i.e., the electric potential destabilizing the film should be almost constant.

The electrocoalescence measurements described above show that the stability of the smectic membranes between the water droplets increases as $T \rightarrow T_{AI}^+$. This behavior is also observed if we study the coarsening of foam-like structures consisting of water droplets separated by thin LC films in a microfluidic device as shown in Fig. 1(d). If the volume fraction of water is sufficiently large compared to that of the LC, the water droplets form a foamlike structure [28] which can show, depending on the temperature, a coarsening with time.

For the study of this coarsening process and its temperature dependence, we prepared a defined foamlike structure at different temperatures and measured for each temperature the time until a certain degree of coarsening, characterized by a certain number of ruptured films in the observed sample volumes, was reached [Fig. 6(a)–6(d)]. Due to the probabilistic nature of the rupture and judging it by our observation, we estimate the error of the characteristic coarsening time to $\pm 20\%$. At $\Delta T = 13.2^\circ\text{C}$ (not shown in the Figure), the water droplets coalesced within ≈ 1 s after contacting each other. This fast coarsening coincides with the results of the previous section at high temperature, i.e., the water droplets are

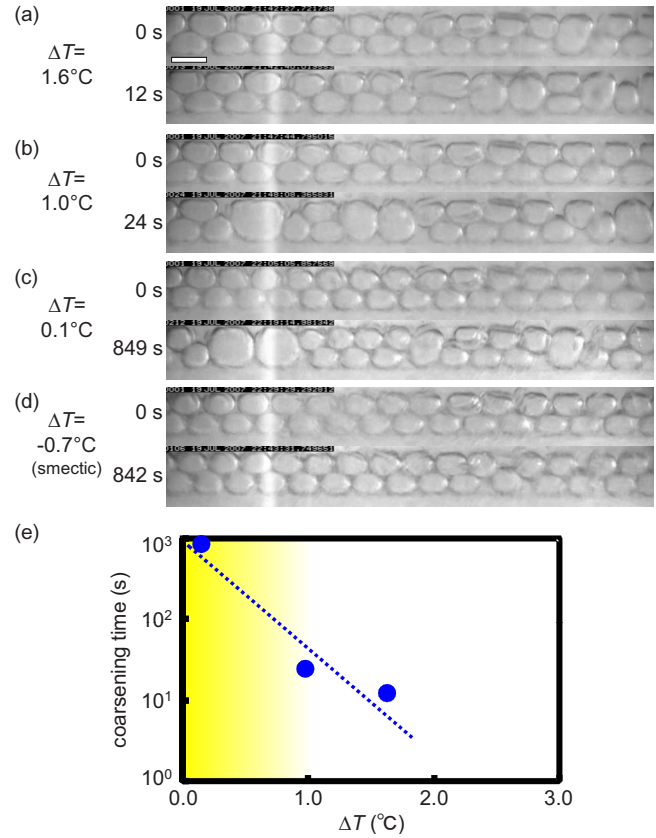


FIG. 6. (Color online) Temperature dependence of the coarsening near the transition temperature to the smectic-A phase, T_{AI} . Images (a) to (c) show for each temperature (indicated beside each image) pairs of micrographs recorded just after the production of the foamlike structure (0 s) and at a similar degree of coarsening. Image (d) demonstrates that no coarsening occurs in the bulk smectic-A temperature range. The channel width is $626 \mu\text{m}$ and the height is $231 \mu\text{m}$. The scale bar corresponds to $500 \mu\text{m}$. (e) Temperature dependence of the characteristic coarsening time resulting from the images (a)–(c). In the shaded temperature range, corresponding to the region where a noticeable difference between V_l and V_r was observed [cf. Fig. 5(e)], the coarsening time increases by two orders of magnitude. The LC sample was 12CB with $\rho_s = 0.034$.

separated by purely isotropic LC films without smectic surface order. At $\Delta T = 1.6^\circ\text{C}$ [Fig. 6(a)] the coarsening took ≈ 12 s. The coarsening time was almost twice as long at $\Delta T = 1.0^\circ\text{C}$ [Fig. 6(b)], and finally it reached more than 10 min at $\Delta T = 0.1^\circ\text{C}$ [Fig. 6(c)]. In Fig. 6(d), the foam was prepared at $\Delta T = 0.1^\circ\text{C}$ and then cooled down to $\Delta T = -0.7^\circ\text{C}$ quickly before coalescence started. In the bulk smectic temperature range, no coarsening was observed even in more than 10 h.

Figure 6(e) shows the temperature dependence of the characteristic coarsening time determined as described above. The coalescence time shows a divergencelike increase as the transition temperature T_{AI} to the bulk smectic-A phase is approached. This observation demonstrates again the relevance of the smectic surface order for the stability of the LC films in the temperature range just above T_{AI} .

IV. CONCLUSION

We have shown that stable macroscopic freely suspended smectic films can be prepared in water with the help of a surfactant that induces homeotropic anchoring of LC molecules at the film/water interfaces. Using optical microscopy and ellipsometry, we have studied the behavior in the temperature region just above the bulk smectic-A-isotropic transition. After the transition to the isotropic phase, thick ($0.1-1\ \mu\text{m}$) films undergo a one-step thinning process down to a thickness of $\approx 30\ \text{nm}$ or less. These thin films consist of smectic layers resulting from surface ordering phenomena. On further heating, an irregular layer-by-layer thinning process is observed until the films rupture $\approx 2\ ^\circ\text{C}$ above the bulk transition. This behavior is different from freely suspended smectic films in air: on heating to the isotropic phase, films in air either just rupture (this is observed for the vast majority of LC compounds) or show a regular layer-by-layer thinning behavior (if the compounds possess partially fluorinated alkyl chains).

Furthermore, we have conducted experiments on smectic membranes separating water droplets in microfluidic channels. Electrocoalescence measurements as well as the coarsening process of LC/water foamlike structures emphasize the important role of the surface ordering at LC/water interfaces for the stability of smectic films in aqueous environment.

Freely suspended smectic films in water can be prepared with different types and different amounts of surfactants. Thus, these systems offer a control over their surface properties that is not possible for freely suspended smectic films in air. The possibility to tune the stability of smectic membranes separating water droplets in microfluidic devices may enable new applications in discrete microfluidics.

ACKNOWLEDGMENTS

This work was partly funded by the Deutsche Forschungsgemeinschaft under Grant No. SFB 755 "Nanoscale Photonic Imaging."

-
- [1] C. Y. Young, R. Pindak, N. A. Clark, and R. B. Meyer, *Phys. Rev. Lett.* **40**, 773 (1978).
- [2] P. Pieranski, L. Beliard, J.-Ph. Tournellec, X. Leoncini, C. Furtlehner, H. Dumoulin, E. Riou, B. Jouvin, J.-P. Fénelon, Ph. Palaric, J. Heuving, B. Cartier, and I. Kraus, *Physica A* **194**, 364 (1993).
- [3] Ch. Bahr, *Int. J. Mod. Phys. B* **8**, 3051 (1994).
- [4] T. Stoebe and C. C. Huang, *Int. J. Mod. Phys. B* **9**, 2285 (1995).
- [5] W. H. de Jeu, B. I. Ostrovskii, and A. N. Shalaginov, *Rev. Mod. Phys.* **75**, 181 (2003).
- [6] D. E. Moncton and R. Pindak, *Phys. Rev. Lett.* **43**, 701 (1979).
- [7] E. B. Sirota, P. S. Pershan, L. B. Sorensen, and J. Collett, *Phys. Rev. A* **36**, 2890 (1987).
- [8] D. R. Link, G. Natale, R. Shao, J. E. Maclennan, N. A. Clark, E. Körblova, and D. M. Walba, *Science* **278**, 1924 (1997).
- [9] P. Mach, R. Pindak, A.-M. Levelut, P. Barois, H. T. Nguyen, H. Baltes, M. Hird, K. Toyne, A. Seed, J. W. Goodby, C. C. Huang, and L. Furenlid, *Phys. Rev. E* **60**, 6793 (1999).
- [10] S. Heinekamp, R. A. Pelcovits, E. Fontes, E. Y. Chen, R. Pindak, and R. B. Meyer, *Phys. Rev. Lett.* **52**, 1017 (1984).
- [11] R. Geer, C. C. Huang, R. Pindak, and J. W. Goodby, *Phys. Rev. Lett.* **63**, 540 (1989).
- [12] C. Y. Chao, T. C. Pan, C. F. Chou, and J. T. Ho, *Phys. Rev. E* **62**, R1485 (2000).
- [13] C. Rosenblatt, R. Pindak, N. A. Clark, and R. B. Meyer, *Phys. Rev. Lett.* **42**, 1220 (1979).
- [14] I. Kraus, Ch. Bahr, I. V. Chikina, and P. Pieranski, *Phys. Rev. E* **58**, 610 (1998).
- [15] A. Fera, I. P. Dolbnya, G. Grübel, H. G. Müller, B. I. Ostrovskii, A. N. Shalaginov, and W. H. de Jeu, *Phys. Rev. Lett.* **85**, 2316 (2000).
- [16] Y. Kimura, N. Kobayashi, and R. Hayakawa, *Phys. Rev. E* **64**, 011705 (2001).
- [17] F. Caillier and P. Oswald, *Phys. Rev. E* **70**, 031704 (2004).
- [18] R. Stannarius, Ch. Bohley, and A. Eremin, *Phys. Rev. Lett.* **97**, 097802 (2006).
- [19] J. M. Brake, A. D. Mezera, and N. L. Abbott, *Langmuir* **19**, 6436 (2003).
- [20] E. Kadivar, Ch. Bahr, and H. Stark, *Phys. Rev. E* **75**, 061711 (2007).
- [21] Ch. Bahr, *Phys. Rev. Lett.* **99**, 057801 (2007).
- [22] Ch. Bahr, *EPL* **88**, 46001 (2009).
- [23] W. Drenckhan, S. J. Cox, G. Delaney, H. Holstea, D. Weaire, and N. Kern, *Colloids Surf., A* **263**, 52 (2005).
- [24] B. M. Ocko, A. Braslau, P. S. Pershan, J. Als-Nielsen, and M. Deutsch, *Phys. Rev. Lett.* **57**, 94 (1986).
- [25] A. J. Leadbetter, J. C. Frost, J. P. Gaughan, G. W. Gray, and A. Mosley, *J. Phys. (France)* **40**, 375 (1979).
- [26] C. Priest, S. Herminghaus, and R. Seemann, *Appl. Phys. Lett.* **89**, 134101 (2006).
- [27] S. Herminghaus, *Phys. Rev. Lett.* **83**, 2359 (1999).
- [28] C. Priest, S. Herminghaus, and R. Seemann, *Appl. Phys. Lett.* **88**, 024106 (2006).
- [29] D. Schlauf, Ch. Bahr, and H. T. Nguyen, *Phys. Rev. E* **60**, 6816 (1999).
- [30] T. Moses, *Phys. Rev. E* **64**, 010702(R) (2001).
- [31] Ch. Bahr and D. Fliegner, *Phys. Rev. A* **46**, 7657 (1992).
- [32] S. Uto, Y. Nakanishi, and T. Matsumoto, *Jpn. J. Appl. Phys., Part 1* **44**, 3170 (2005).
- [33] S. Okuda and S. Uto, *Jpn. J. Appl. Phys., Part 1* **45**, 5889 (2006).
- [34] T. Stoebe, P. Mach, and C. C. Huang, *Phys. Rev. Lett.* **73**, 1384 (1994).
- [35] K. Kočevar, A. Borštnik, I. Muševič, and S. Žumer, *Phys. Rev. Lett.* **86**, 5914 (2001).